Assessment of Vecuronium Quality Using Near-Infrared Spectrometry

James T. Isaacs[1], Philip J. Almeter[1, 2], Aaron N. Hunter[1], Thomas A. Lyman[1], Stephanie P. Zapata[1], Bradley S. Henderson[1], Seth A. Larkin[1, 2], Lindsey M. Long[1, 2], Megan N. Bossle[1, 2], Smaran A. Bhaktawara[1, 2], Matthew F. Warren[1, 2], Austin M. Lozier[1, 2], Joshua D. Melson[1, 2], Savannah R. Fraley[1, 2], Eunice Hazzel L. Relucio[1, 2], Margaret A. Felix[1], Jeffrey W. Reynolds[3], Ryan W. Naseman[1, 2], Thomas L. Platt[1, 2], Robert A. Lodder[4,*]

University of Kentucky
Lexington, KY

1. Department of Pharmacy Services, University of Kentucky HealthCare, Lexington, KY 40536
2. Pharmacy Practice & Sciences, College of Pharmacy, University of Kentucky, Lexington, KY 40536
3. Department of Finance, University of Kentucky HealthCare, Lexington, KY
4. Department of Pharmaceutical Sciences, University of Kentucky, Lexington, KY 40536

*Author to whom correspondence should be addressed. Email: Lodder @ g.uky.edu
ORCID 0000-0001-6133-7561

RAPID COMMUNICATION

Abstract

This study employed Fourier Transform near-infrared spectrometry to assess the quality of vecuronium bromide, a neuromuscular blocking agent. Spectral data from two lots of vecuronium were collected and analyzed using the BEST metric, principal component analysis (PCA) and other statistical techniques. The results showed that there was variability between the two lots and within each lot. Several outliers in the spectral data suggested potential differences in the chemical composition or sample condition of the vials. The outliers were identified and their spectral features were examined. A total of eight unique outliers were found in the PC space from PCs 1 to 9, so 22% of the total vials were outliers. The study findings suggest that the manufacturing process of vecuronium bromide may have been operating

outside of a state of process control. Further investigation is needed to determine the source of these variations and their impact on the safety and efficacy of the drug product.

Introduction

The University of Kentucky's (UK) Drug Quality Task Force (DQTF) was established in August of 2019 to engage in consumer-level quality assurance screening for drugs used within UK HealthCare's pharmacies (Isaacs, 2023a). The DQTF currently screens medications using Fourier transform near-infrared spectrometry (FTNIR) and Raman spectrometry for potential quality defects indicated by variability in absorbance peak intensities and locations. Through years of continuous monitoring, DQTF has assembled a spectral library containing medications typically used in a health system setting. Statistical analyses using the DQTF spectral library are performed to identify potential intra-lot and inter-lot variability in medications under review. Using Medwatch and publications in the scientific literature, the DQTF reports its findings in an effort to hold manufacturers accountable for GMP requirements and to improve patient outcomes by providing information on quality to augment the information on price that is already available. The increasing transparency is designed to improve the pharmaceutical supply chain.

Drug Product

Vecuronium Bromide for Injection is a neuromuscular blocking agent with an intermediate duration of action. The medication comes in vials as a sterile, nonpyrogenic freeze-dried cake made up of very fine microscopic crystalline particles. It is intended for intravenous use only. Each 10 mg vial also contains citric acid anhydrous (20.75 mg), sodium phosphate dibasic anhydrous (16.25 mg), mannitol (97 mg), and sodium hydroxide and/or phosphoric acid to maintain a pH range of 3.5 to 4.5. Vecuronium bromide is used as a supplement to general anesthesia to aid in endotracheal intubation and to induce muscle relaxation during surgery or mechanical ventilation (see Figure 1)(FDA Access Data, 2018).

Figure 1. Photo of vials of the vecuronium bromide drug product.

The lot numbers making up the spectral library were 41576CA and 41580CA.

Background

Vecuronium bromide is being used in current research. Succinylcholine-induced fasciculation (muscle twitching) and postoperative myalgia (muscle pain) are common side effects of anesthesia. Vecuronium bromide and preservative-free 2% plain lignocaine hydrochloride have been shown to reduce these side effects (Bayable, 2023). This study compared the effectiveness of these two drugs in preventing succinylcholine-induced fasciculation and postoperative myalgia. The study found that vecuronium bromide was more effective at preventing succinylcholine-induced fasciculation. Preservative-free 2% plain lignocaine hydrochloride was more effective at preventing postoperative myalgia. These findings suggest that both drugs may be useful for preventing these side effects.

Vecuronium bromide is used in executions. Tennessee's use of the sedative midazolam in lethal injections has been the subject of controversy, with critics arguing that the drug is not effective at rendering inmates unconscious and that it can cause them to experience excruciating pain (Crocker, 2023). In 2018, the state of Tennessee executed Billy Ray Irick by lethal injection using midazolam, vecuronium bromide, and potassium chloride. After the execution, witnesses reported that Irick gasped and convulsed for several minutes, suggesting that he was not fully unconscious when the other two drugs were administered. In response to the outcry over Irick's execution, Tennessee revised its lethal injection protocol to require that midazolam be administered in combination with a paralytic agent, such as vecuronium bromide. However, this change did not address the concerns of critics, who argue that vecuronium bromide can also cause pain and suffering. In addition, Tennessee's lethal injection protocol does not require that the drugs be administered by a qualified anesthesiologist, which critics argue is necessary to ensure that the drugs are administered properly and that the inmate does not experience pain.

Recalls

Vecuronium bromide supply has been disrupted multiple times recently (FDA Drug Shortages, 2023). In June 2020 the U.S. Food and Drug Administration (FDA) issued an alert regarding the temporary absence of a warning statement on the vial caps of vecuronium bromide. This absence was due to a manufacturing error, which prompted the FDA to stress the importance of visually inspecting the vial labels. These potent drugs were used in various medical procedures and could cause serious harm or death if used inappropriately. The warning statement, usually present on the vial caps, cautioned healthcare professionals not to use these drugs without the requisite ability to manage a patient's airway and ventilation. The FDA had been working with manufacturers, Pfizer and Fresenius Kabi, to rectify this issue. The affected products were expected to be in circulation until mid-2024. The FDA encouraged reporting of any adverse events related to these products. The agency also took steps to prevent similar occurrences in the future. Healthcare professionals were urged to be vigilant and to report any issues to the FDA's MedWatch Safety Information and Adverse Event Reporting Program.

Shortages

According to the ASHP Drug Shortage List (ASHP, 2023), several versions of vecuronium bromide are currently experiencing shortages. Fresenius Kabi's 10 mg vials have a limited supply with expiration dates less than 5 months away. Hikma's 10 mg and 20 mg vials are on backorder with no specific reason provided for the shortage. The estimated resupply for Hikma's 10 mg vials is the second quarter of 2024, while no estimated release date is available for Hikma's 20 mg vials.

Vecuronium Bromide Injection is currently listed as in shortage on the FDA website, too (FDA Drug Shortages, 2023). Hospira, Inc. 1 mg/1 mL vials are available. Eugia US LLC's 10 mg and 20 mg vials are available but with sporadic availability expected. Fresenius Kabi USA, LLC's 1 mg/1 mL vials are available with 6-month expiry dating by request, while the 20 mg vials are not available at this time. Mylan Institutional 10 mg and 20 mg vials are available. The reasons for the shortages vary depending on the manufacturer, including delay in shipping of the drug (Fresenius Kabi USA) and demand increase for the drug (Mylan).

FDA Medwatch

An FDA Form 3500 Medwatch describing the findings of this Rapid Communication was filed.

Methods

FTNIR (Fourier Transform Near-Infrared) Spectrometry

Using nondestructive analytical techniques, FTNIR spectra were collected from inventory as part of routine medication quality screening. A representative sample of individual vials were selected for screening and noted to be stored under the conditions required by the manufacturer in their original packaging. FTNIR spectra were collected noninvasively and nondestructively through the bottom of the vials using a Thermo Scientific Antaris II FTNIR Analyzer (Waltham, MA, USA)(Felix, 2023b).

Smoothing

Data smoothing is a technique used to remove noise from data. This can be done by fitting a smooth curve to the data, such as a cubic spline. Cubic splines are piecewise cubic polynomials that are continuous and have continuous first and second derivatives. This makes them very smooth and resistant to noise. Cubic splines can be easily fitted to data using least squares (Matlab, 2023)(Pollock, 1998).

Multiplicative Scatter Correction (MSC)

Multiplicative scatter correction (MSC) is a widely used spectrometric normalization technique. Its purpose is to correct spectra in such a way that they are as close as possible to a reference spectrum, generally the mean of the data set, by changing the scale and the offset of the spectra (Isaksson, 1988).

BEST (Bootstrap Error-Adjusted Single-sample Technique)

The BEST calculates distances in multidimensional, asymmetric, nonparametric central 68% confidence intervals in spectral hyperspace (roughly equivalent to standard deviations)(Dempsey, 1996). The BEST metric can be thought of as a "rubber yardstick" with a nail at the center (the mean). The stretch of the yardstick in one direction is therefore independent of the stretch in the other direction. This independence enables the BEST metric to describe odd shapes in spectral hyperspace (spectral point clusters that are not multivariate normal, such as the calibration spectra of many biological systems). BEST distances can be correlated to sample composition to produce a quantitative calibration, or simply used to identify similar regions in a spectral image. The BEST automatically detects samples and situations unlike any encountered in the original calibration, making it more accurate in chemical investigation than typical regression approaches to near-IR analysis. The BEST produces accurate distances even when the number of calibration samples is less than the number of wavelengths used in calibration, in contrast to other metrics that require matrix factorization. The BEST is much faster to calculate as well (O(n) instead of the $O(n^3)$ required by matrix factorization.

Principal Components (PCs)

Principal component analysis is the process of computing the principal components of a dataset and using them to execute a change of basis (change of coordinate system) on the data, usually employing only the first few principal components and disregarding the rest (Joliffe, 2016). PCA is used in exploratory data analysis and in constructing predictive models. PCA is commonly utilized for dimensionality reduction by projecting each data point onto only the first few principal components to obtain lower-dimensional data while preserving as much of the original variation in the data as possible. The first principal component is the direction that maximizes the variance of the projected data. The second principal component is the direction of the largest variance orthogonal to the first principal component. Decomposition of the variance typically continues orthogonally in this manner until some residual variance criterion is met. Plots of PC scores help reveal underlying structure in data.

Subcluster Detection

In typical near-infrared multivariate statistical analyses, samples with similar spectra produce points that cluster in a certain region of spectral hyperspace. These dusters can vary significantly in shape and size due to variation in sample packings, particle-size distributions, component concentrations, and drift with time. These factors, when combined with discriminant analysis using simple distance metrics, produce a test in which a result that places a particular point inside a particular cluster does not necessarily mean that the point is actually a member of the cluster. Instead, the point may be a member of a new, slightly different cluster that overlaps the first. A new cluster can be created by factors like low-level contamination, moisture uptake, or instrumental drift. An extension added to part of the BEST, called FSOB (Fast Son of BEST) can be used to set nonparametric probability-density contours inside spectral clusters as well as outside (Isaacs, 2023c)(Lodder, 1988), and when multiple points begin to appear in a certain region of cluster-hyperspace the perturbation of these density contours can be detected at an assigned significance level using r values, and visualized using quantile-quantile (QQ) plots. The detection of unusual samples both within and beyond 3 SDs of the center of the training set is possible with this method. Within the ordinary 3 SD limit, however, multiple instances are needed to detect unusual samples with statistical significance.

Artificial Intelligence Tools

Artificial intelligence (AI) tools, principally used for background information, include Bard (Google LLC) and GPT-4 (OpenAI). AI can be used in a variety of ways, including to brainstorm, organize thoughts, develop arguments, and edit.

Results and Discussion

Interlot analysis

Smoothed, scatter-corrected full near-IR spectra of the two lots in the library appear in Figure 2.

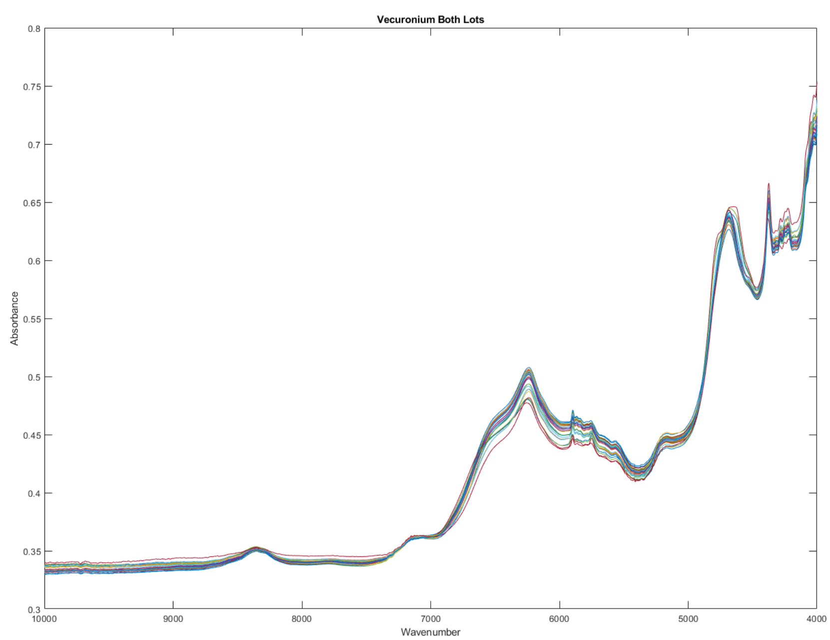

Figure 2. Smoothed graphs of 36 spectra in the library formed by the two lots

Most of the differences that are observable at the scale shown in Figure 2 between the library spectra are visible between 4000 and 5000 cm^{-1}.

PC Plots

Principal component score scatterplots offer valuable insights into your data structure and relationships between samples by visually representing their projections onto specific principal components. Scatter plots of the first few PCs reveal how data points are distributed in the reduced-dimensionality space. Clusters of points indicate similar samples, while outliers stand out as distant points, potentially representing unique or anomalous cases. Scatter plots can showcase gradual transitions or trends within your data. PC plots provide a better view of the magnitude and types of differences between the vials. Scatterplots can highlight which PCs capture specific aspects of the data. For instance, plotting a variable (e.g., API concentration) against a PC score might reveal how that variable contributes to the variance captured by that component. Figure 3 shows a PC plot of the 36 vials taken from the two lots of vecuronium bromide to form the spectral library. Eighteen spectra were collected from 18 vials from each lot number. Most of the outliers were in the second lot. Table 1 shows the total and cumulative spectral variation accounted for by each of the first nine principal components of the spectra in the library. The relatively low variation accounted for by the first principal component suggests that there may be more than the usual amount of variation for a pharmaceutical within the spectral library.

Table 1: Variation accounted for by each of the principal components of the spectra in the library

PC Number	Variation in this PC	Cumulative PC Variation
1	0.7418	0.7418
2	0.1141	0.8559
3	0.0915	0.9474
4	0.0286	0.9760
5	0.0121	0.9882
6	0.0057	0.9939
7	0.0031	0.9970
8	0.0011	0.9981
9	0.0008	0.9988

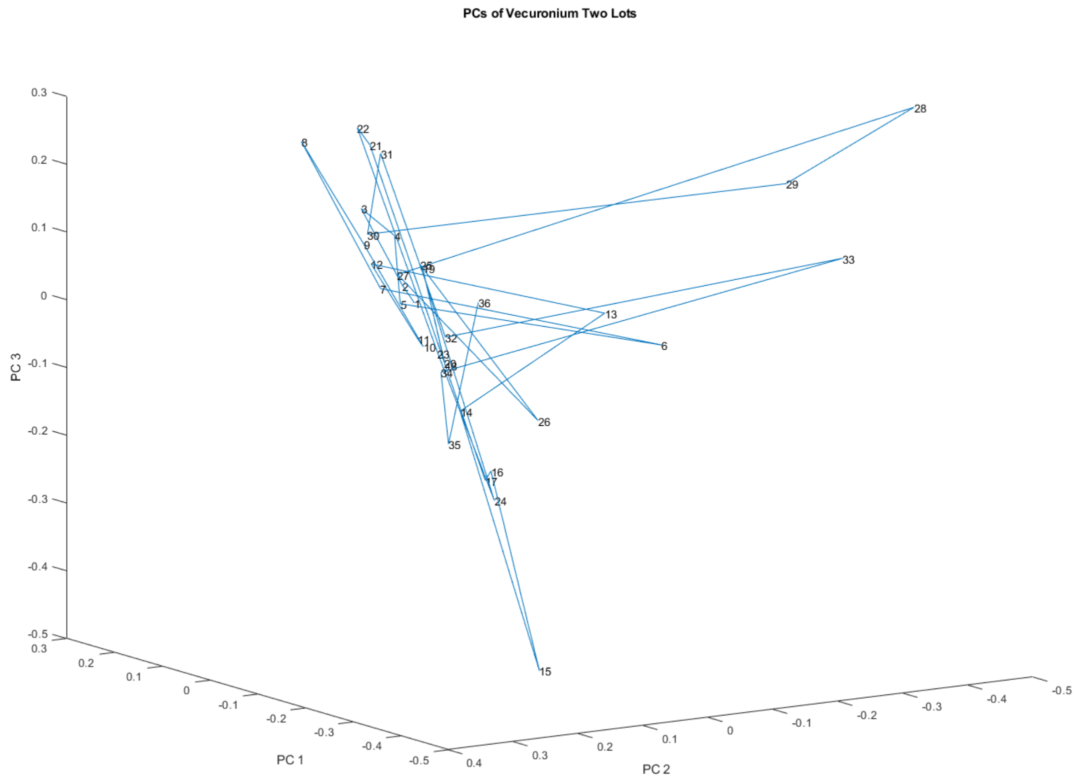

Figure 3. PC plot of the spectra of 36 vials in the library. Vials 28, 29, and 33 appear to be possible outliers. Vial 15 might be an outlier as well.

Figure 3 shows the PC plot of the spectral library using the first three PCs. In this rotation, vials 28, 29, and 33 appear to be possible outliers. Vial 15 could be an outlier as well, but it appears to be displaced along the major axis of the library cluster, which would reduce its distance in SDs from the center of the library in comparison to vials like 28, 29, and 33, which have a similar Euclidean distance from the library. Vials 28, 29, and 33 are displaced along a minor axis. The SD in the direction of this minor axis is smaller, so the Euclidean distance scaled by this SD is larger than the similar distance to vial 15 scaled by a larger SD.

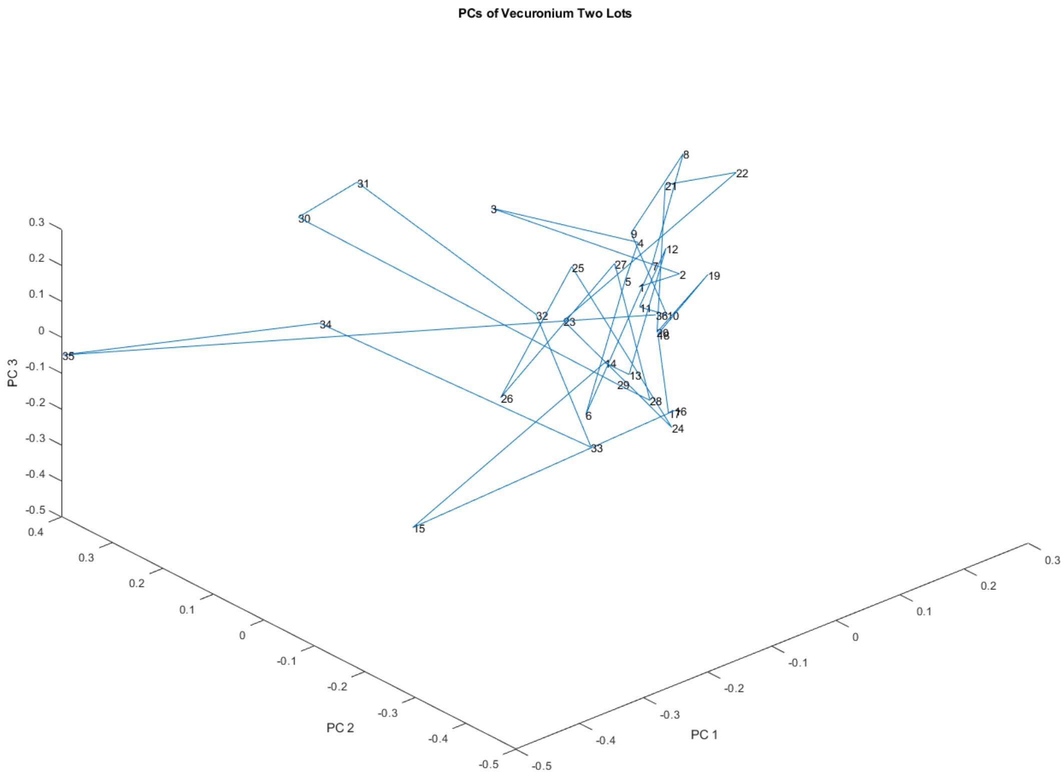

Figure 4. Another rotation of the PC plot of the spectra of 36 vials in the library (compare to Figure 3). In this rotation vial 35 looks like the only possible outlier.

Other rotations of the library in the same space reveal other vials displaced from the center of the library in different directions. In Figure 4, vial 35 looks like the only possible outlier. In Figure 5, vials 28, 29, 33, 31, 30, 34, and 35 all appear to be outliers.

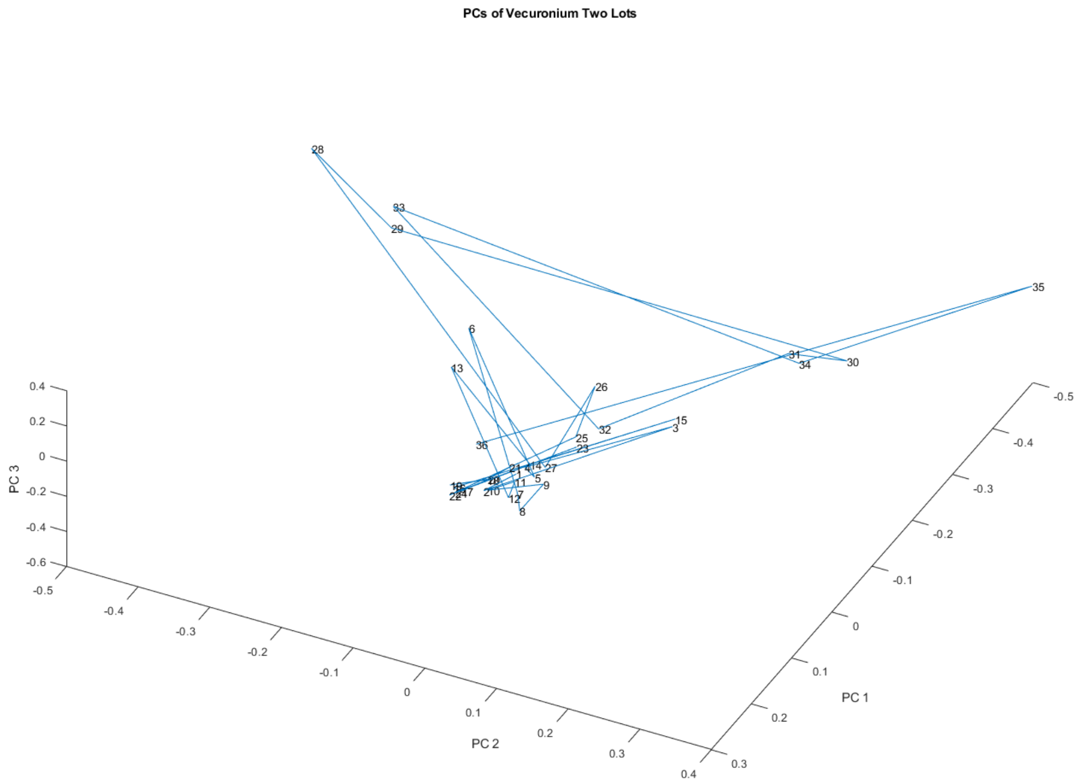

Figure 5. Another rotation of the PC plot of the spectra of 36 vials in the library (compare to Figure 3 and Figure 4). In this rotation, vials 28, 29, 33 and vials 31, 30, 34, and 35 all appear to be possible outliers. Vials 28 and 35 are orthogonal outliers, so the chemical changes occurring in them and other vials in the same direction (3, 15, 30, 31, and 34 for vial 35, and 6, 13, 29, 33) might be completely different.

The actual outliers by distance in BEST SDs measured using the first three PCs are vial 15 (3.9 SDs from the center of the library, which is near vial 11), vial 28, (5.0 SDs), and vial 35 (5.0 SDs). Vial 11 is used for comparisons with the outliers in Figure 6, Figure 7, and Figure 8 because it is near the center of the library.

There are three outliers measured on PCs 1 through 3. Therefore, 8% of the vials are unusual on the first three PCs.

 DOI:10.6084/m9.figshare.24846285 CIC Pharmaceutical Sciences
ISSN: 1547-8890

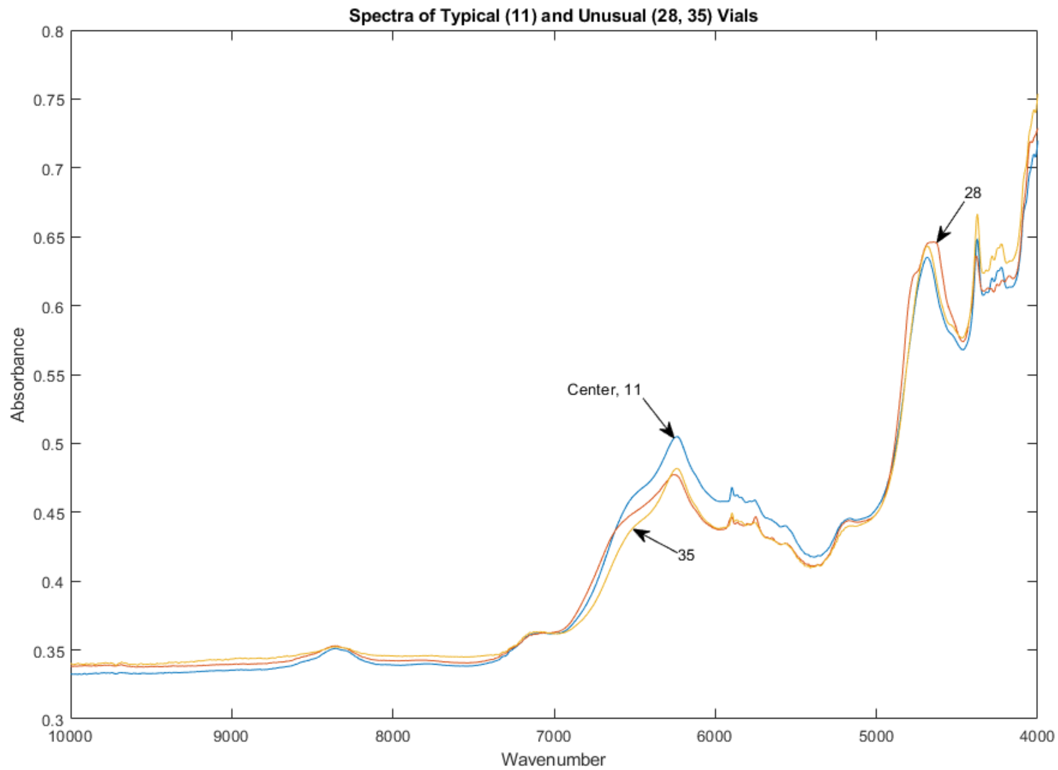

Figure 6. Representative spectra of typical and unusual vials of vecuronium in the library. The typical vial is shown in the blue graph of vial 11. The potential outliers are vials 28 (red) and 35 (yellow). Compare these with Figure 3, Figure 4, and Figure 5.

Figure 6 depicts the typical spectra of vecuronium in the blue line (vial 11), and the unusual spectra with the red line (vial 28) and the yellow line (vial 35). The zoomed in images show the changes better. Figure 7 zooms in on the region from 5700 to 5950 cm^{-1}. In this figure, vial 28 sticks out from the rest as the most unusual, with a large peak around 5750 cm^{-1} that the other vials do not have. In addition, vial 28 has a peak at about 5800 cm^{-1} that the other vials do not have, and a smaller peak at around 5840 cm^{-1} than the other 3 vials (11, 15, and 35) show.

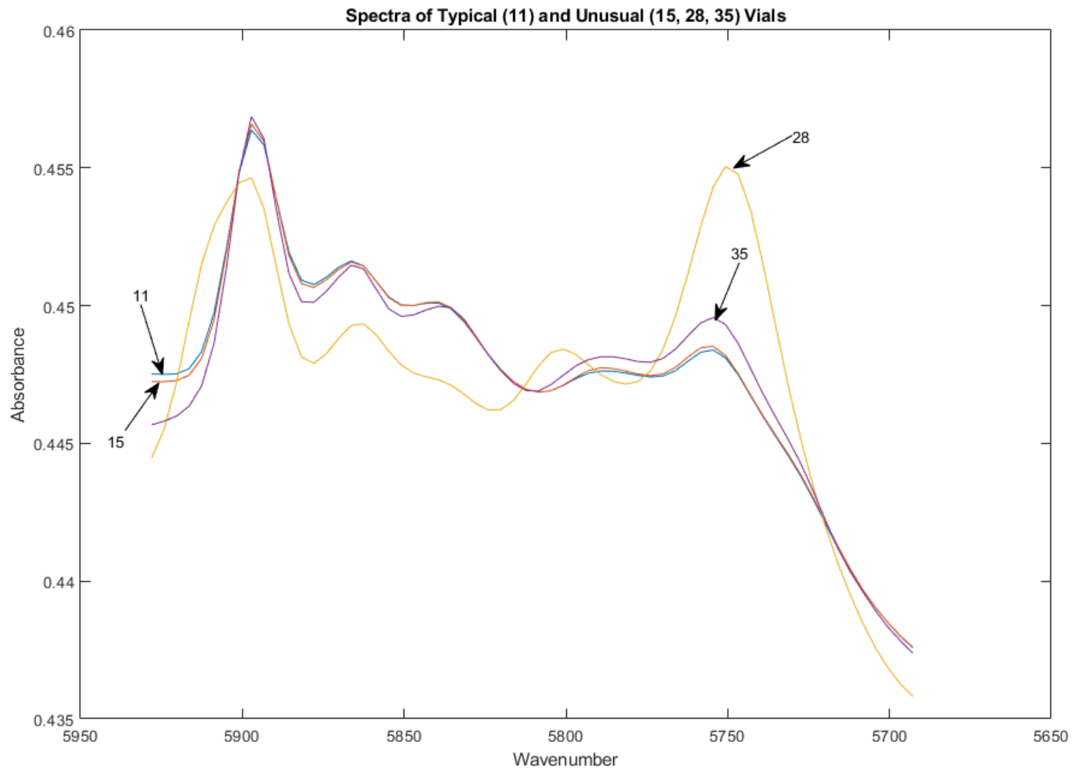

Figure 7. A zoom in on the region from 5650 to 5950 cm^{-1} shown in Figure 6. The spectrum of vial 15 is added.

Figure 8 zooms in on the region from 4200 cm^{-1} to 4800 cm^{-1}. In this region, vial 28 (yellow line) has differences from the other unusual vials at about 4250, 4520, 4620, and 4780 cm^{-1}. The peak shoulder at about 4530 cm^{-1} is different in all of the unusual spectra.

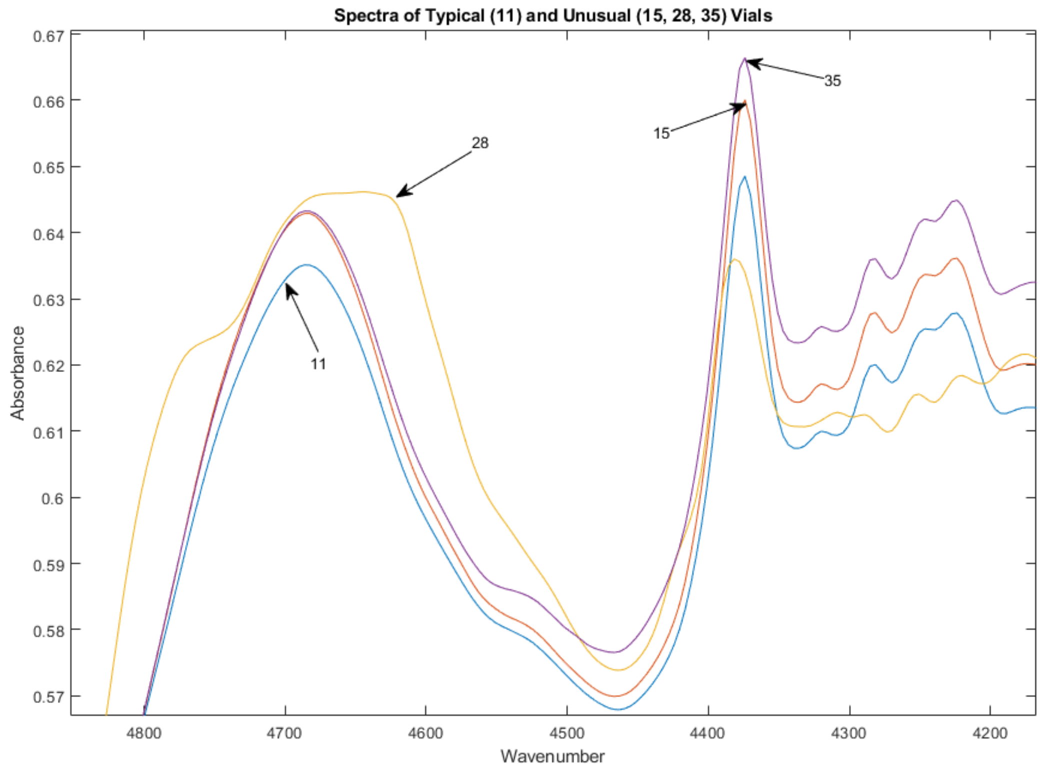

Figure 8. A zoom in on the region from 4200 to 4800 cm^{-1} shown in Figure 6. The same vials are depicted as those that appear in Figure 7 (vials 11, 15, 28, and 35)

Figure 9 moves past the first three PCs to plot the library spectra on PCs 4, 5, and 6. There are three outliers on PCs 4 to 6, so 8% of the vials are unusual on PCs 4 through 6. These outlier vials are different from the vials identified as unusual in the first three PCs. Vial 8, which does not look very unusual in Figure 9, is actually an outlier in another rotation of PCs 4, 5, and 6.

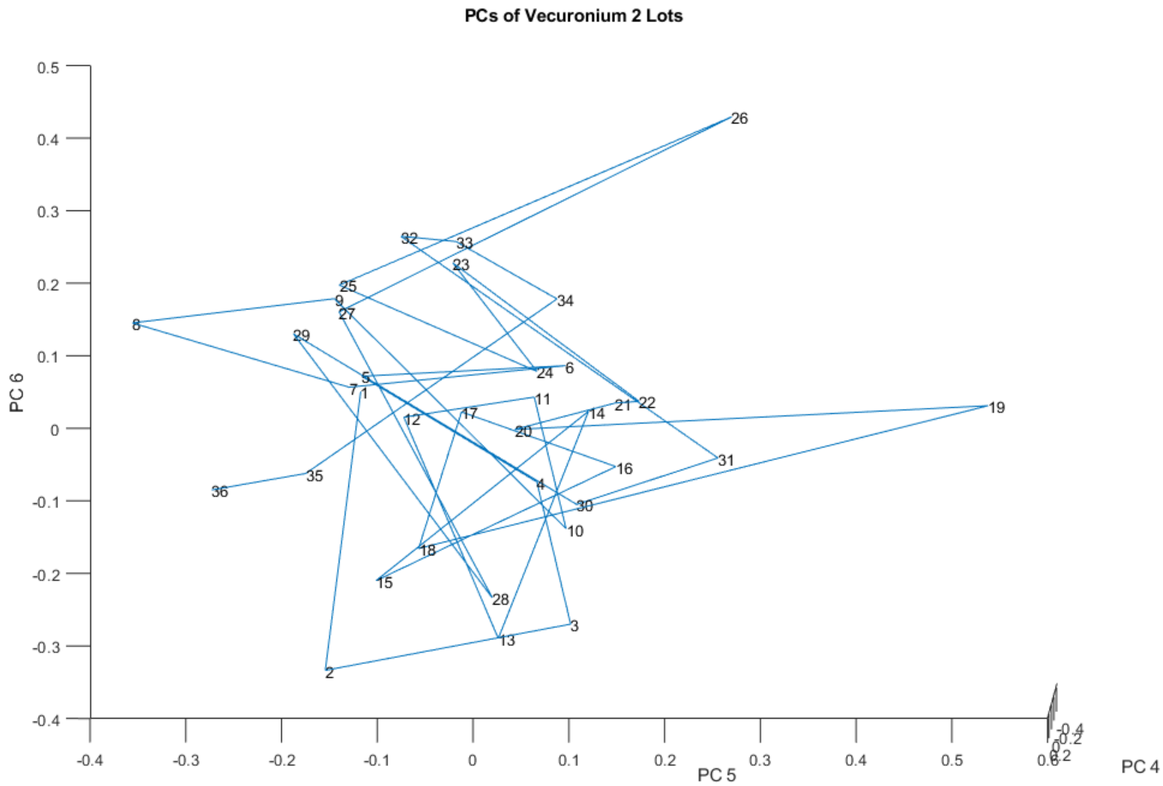

Figure 9. A plot of the spectra in the library on PCs 4, 5, and 6. Vials 19 (4.1 SDs) and 26 (3.6 SDs) are outliers.Vial 8 is an outlier in another rotation (3.6 SDs).

Figure 10 moves on to the next set of three lower PCs, PCs 7, 8, and 9. Vials 27 (4.2 SDs) and 36 (3.5 SDs) are outliers in PCs 7 through 9. These principal components contain substantial spectral noise. Altogether there are a total of eight unique outliers in the PC space from 1 to 9, so 22% of the vials are outliers. If the noisiest PCs are ignored (PCs 7 to 9), 17% of the vials are outliers.

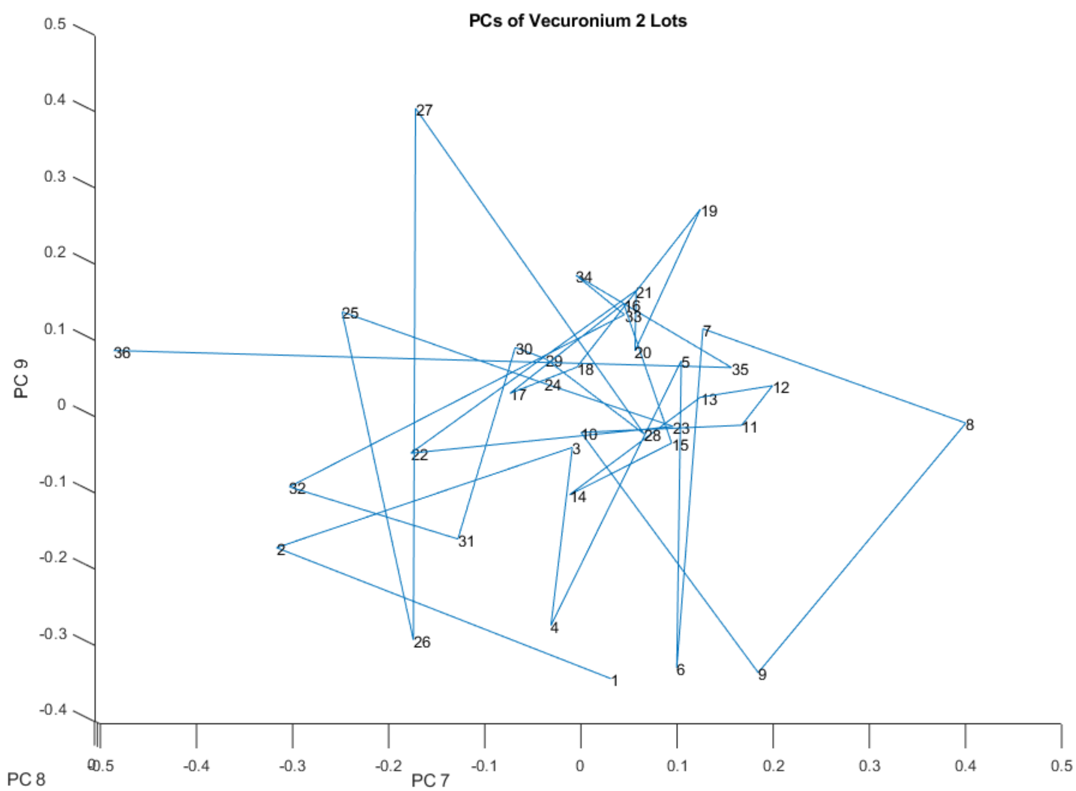

Figure 10. A plot of the spectra in the library on PCs 7 , 8, and 9. Vials 27 (4.2 SDs) and 36 (3.5 SDs) are outliers in PCs 7 through 9. These principal components contain substantial noise, however.

PC Loadings

Each PC represents a hidden factor explaining specific variations in the spectra. Analyzing the loading signs and peaks/valleys helps interpret what these factors represent (e.g., chemical composition, sample condition, instrumental effects). High loading values pinpoint specific wavelengths or features within the spectra that are most relevant for explaining the captured variance. Plotting PC loadings as spectra allows visualization of how different scores on a specific PC translate to changes in the actual spectra. Low loading values often indicate noise or less informative spectral features. This helps focus analysis on meaningful variations.

Figure 11 shows the loadings of the first principal component for two lots of the chemical compound vecuronium forming the spectral library. The x-axis represents the wavenumber (in cm^{-1}) of the near-infrared spectra, and the y-axis represents the loading values for PC 1. The peaks and valleys in the loading plot indicate the wavenumbers at which the infrared spectrum varies the most in order to capture the differences between the two lots of vecuronium.

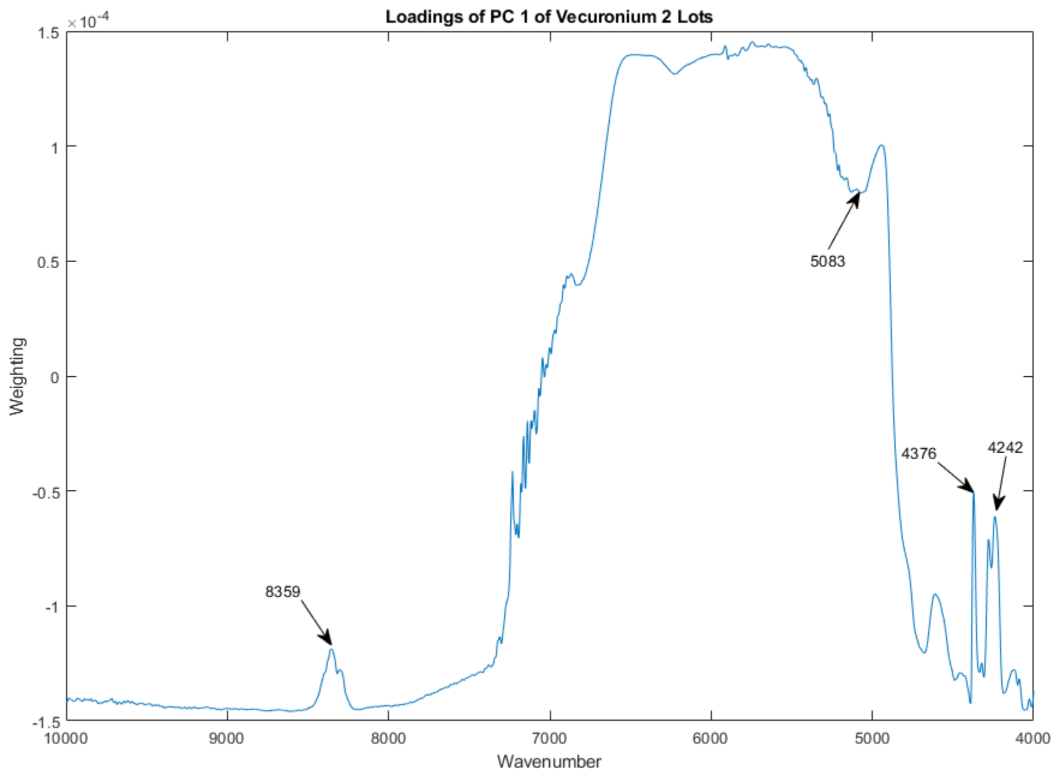

Figure 11. A graph of the loadings of PC 1 of the spectral library. Important spectral features are marked at 4242, 4376, 5083, and 8359 cm^{-1}.

Figure 12 is a graph of the loadings of PC 2 of the spectral library. Important spectral features are marked at 4242, 4838, 6743, 7145, and 8366 cm^{-1}.

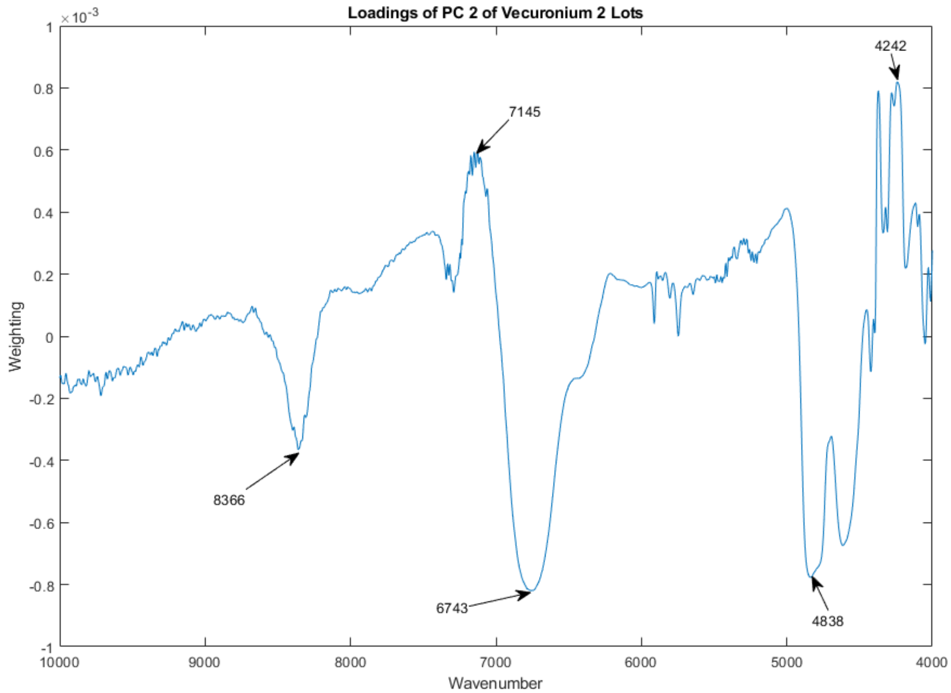

Figure 12. A graph of the loadings of PC 2 of the spectral library.

Figure 13 is a graph of the loadings of PC 3 of the spectral library. Important spectral features are marked at 4361, 4718, 4890, 6237, 6951, and 7242 cm^{-1}.

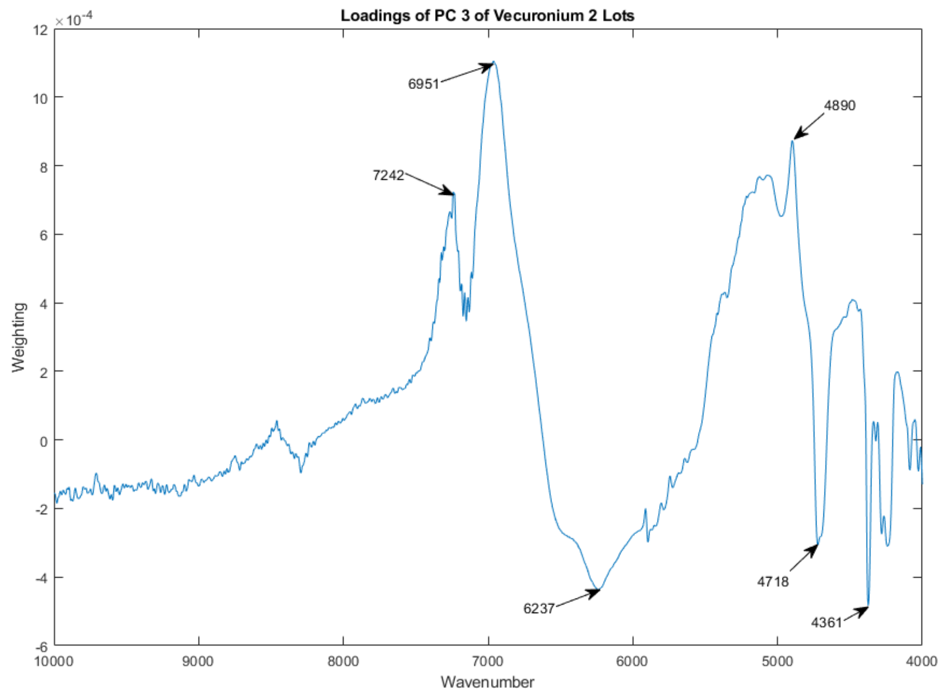

Figure 13. A graph of the loadings of PC 3 of the spectral library.

Figure 14 is a graph of the loadings of PC 3 of the spectral library. Important spectral features are marked at 4890, 5187, 7063, 7302, and 8366 cm^{-1}. Noise can be seen creeping into the spectra from the left (high wavenumber) number side.

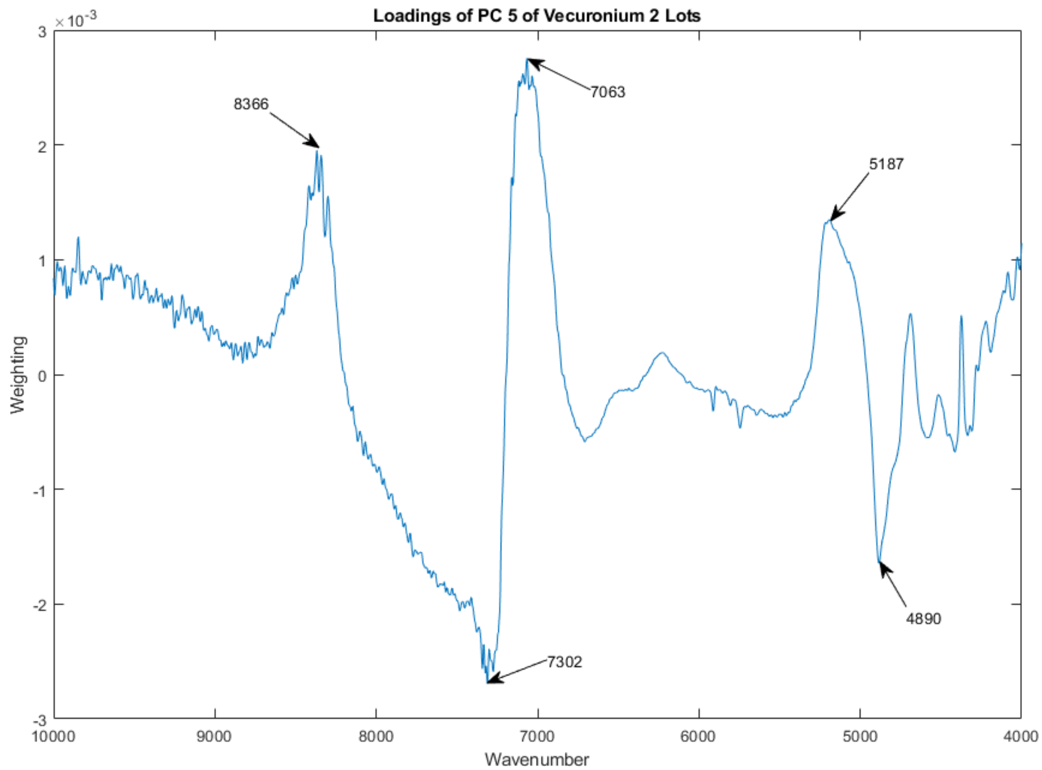

Figure 14. A graph of the loadings of PC 3 of the spectral library.

Figure 15 shows a graph of the loadings of PC 4 of the spectral library. Important spectral features are marked at 4696, 5187, 7153, and 8351 cm^{-1}. Interestingly, the noise at the left hand side of the spectrum seems to be reduced in Figure 15 from what was observed on the left side of Figure 14.

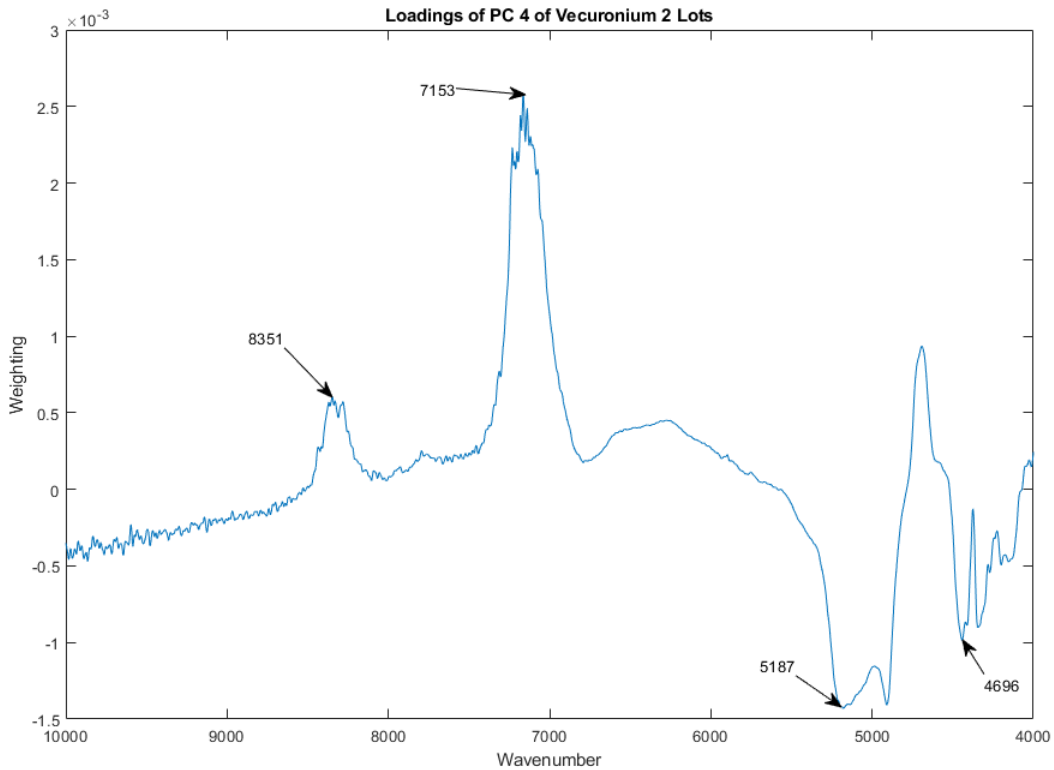

Figure 15. A graph of the loadings of PC 4 of the spectral library.

Figure 16 is a plot of the loadings of PC 6 of the spectral library. Major spectral features are marked at 4346, 4443, 4726, 5202, 7004, 7220, and 8359 cm^{-1}. The noise on the left hand side of the spectrum appears to be increasing again in Figure 16 compared to Figure 15.

 DOI:10.6084/m9.figshare.24846285 *CIC Pharmaceutical Sciences*
ISSN: 1547-8890

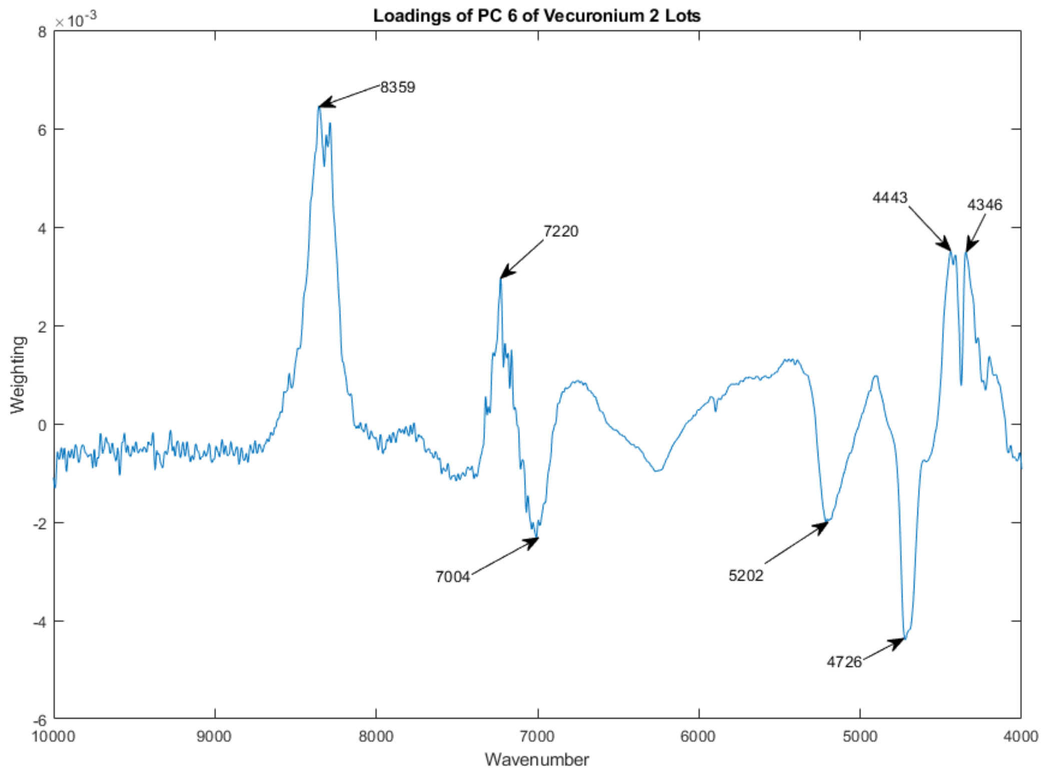

Figure 16. A graph of the loadings of PC 6 of the spectral library.

Figure 17 depicts the graph of the loadings of PC 7 of the spectral library. Relevant spectral features are marked at 4145, 4376, 4495, 4718, 5180, 7145, and 8314 cm^{-1}.

 DOI:10.6084/m9.figshare.24846285 CIC Pharmaceutical Sciences
ISSN: 1547-8890

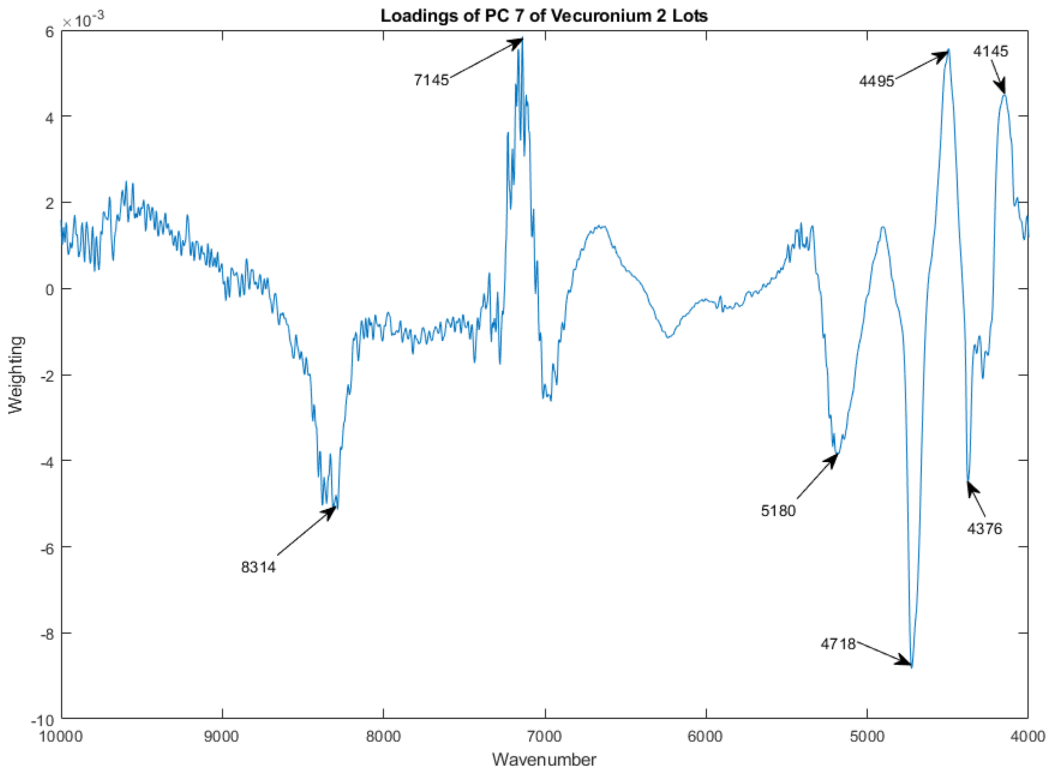

Figure 17. A graph of the loadings of PC 7 of the spectral library.

Figure 18 is a graph of the loadings of PC 8 of the spectral library. Dominant spectral features are marked at 4361, 4726, 5187, 5366, 6929, and 7078 cm^{-1}.

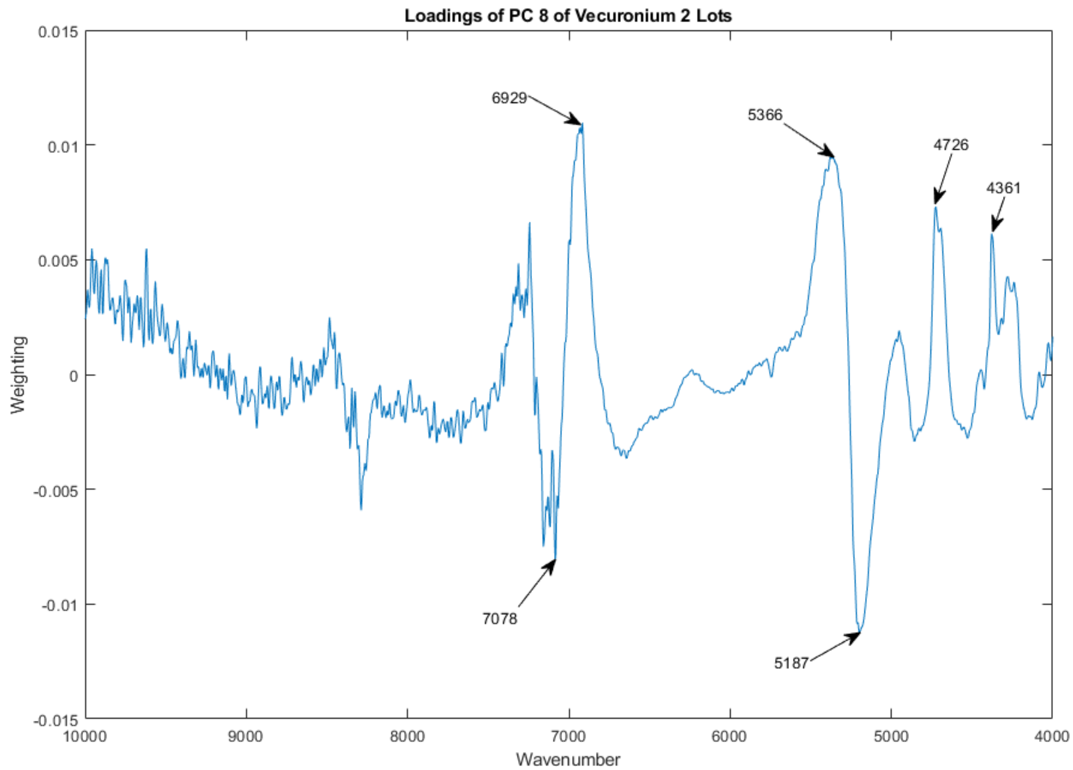

Figure 18. A graph of the loadings of PC 8 of the spectral library.

Figure 19 shows a graph of the loadings of PC 9 of the spectral library. The foremost spectral features are marked at 4346, 4495, 5202, and 7227 cm^{-1}.

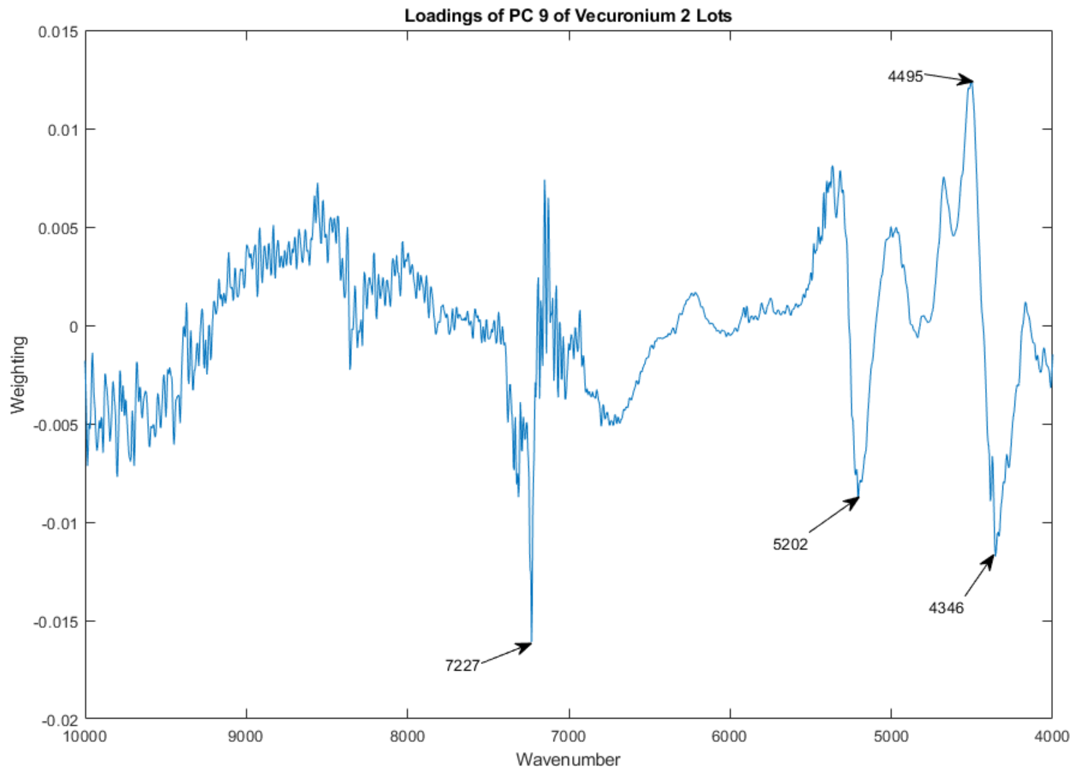

Figure 19. A graph of the loadings of PC 9 of the spectral library.

Conclusion

Vecuronium Bromide for Injection is a neuromuscular blocking agent with an intermediate duration of action. The medication comes in vials as a sterile, nonpyrogenic freeze-dried cake made up of very fine microscopic crystalline particles. It is intended for intravenous use only. Each 10 mg vial also contains citric acid anhydrous (20.75 mg), sodium phosphate dibasic anhydrous (16.25 mg), mannitol (97 mg), and sodium hydroxide and/or phosphoric acid to maintain a pH range of 3.5 to 4.5. Vecuronium bromide is used as a supplement to general anesthesia to aid in endotracheal intubation and to induce muscle relaxation during surgery or mechanical ventilation.

Intralot variability was measured in a library of two lots of vecuronium bromide using FT-NIR spectrometry. A total of eight unique outliers were found in the PC space from PCs 1 to 9, so 22% of the vials are outliers. If the noisiest PCs are ignored (PCs 7 to 9), 17% of the vials are outliers.

Based on the collected spectral data, statistical analysis, and PC score scatterplots, variability was observed within the different lots of vecuronium bromide that were analyzed. Several outliers were detected, indicating potential differences in the chemical composition or sample condition of the vials. The concern is that certain vials could contain impurities or adulterants. These spectrometric results do not prove an excess level of impurities or adulteration. However, they suggest that the manufacturing process may have been operating outside of a state of process control. Additional investigation is needed.

Acknowledgements

The project described was supported in part by the National Center for Research Resources and the National Center for Advancing Translational Sciences, National Institutes of Health, through Grant UL1TR001998. The content is solely the responsibility of the authors and does not necessarily represent the official views of the NIH.

References

ASHP, 2023. Vecuronium Bromide Injection. https://www.ashp.org/drug-shortages/current-shortages/drug-shortage-detail.aspx, retrieved Nov. 25, 2023

Bayable, S. D., Ayenew, N. T., Misganaw, A., Fetene, M. B., & Amberbir, W. D. (2023). The Effects of Prophylactic Intravenous Lignocaine vs Vecuronium on Succinylcholine-Induced Fasciculation and Postoperative Myalgia in Patients Undergoing Elective Surgery at Debre Markos Comprehensive Specialized Hospital, Ethiopia, 2022: Prospective Cohort Study. International Journal of General Medicine, 2663-2670.

Crocker, A., Gunn, J., Li, A. R., & Tackeff, M. (2023) Tennessee Suspends Executions And Authorizes Independent Investigation Of Lethal Injection Protocol. Amicus Journal,, Issue 44, 22-28. https://www.bassberry.com/wp-content/uploads/lethal-injection-protocol-tennessee.pdf

Dempsey, R. J., Davis, D. G., Buice Jr, R. G., & Lodder, R. A. (1996). Biological and medical applications of near-infrared spectrometry. Applied Spectroscopy, 50(2), 18A-34A.

FDA Access Data, 2018. Vecuronium Bromide For Injection, https://www.accessdata.fda.gov/drugsatfda_docs/label/2018/075549s013lbl.pdf, retrieved Nov. 15, 2023

FDA Drug Shortages, 2023. Current and Resolved Drug Shortages and Discontinuations Reported to FDA, Vecuronium Bromide Injection. https://www.accessdata.fda.gov/scripts/drugshortages/dsp_ActiveIngredientDetails.cfm

Isaacs, J. T., Almeter, P. J., Henderson, B. S., Hunter, A. N., Lyman, T.A. Zapata, S. P., Henderson, B. S., Larkin, S. A., Long, L. M., Bossle, M. N., Bhaktawara, S. A., Warren, M. F., Lozier, A. M., Melson, J. D., Fraley, S. R., Relucio, E. H. L., Felix, M. A., Reynolds, J. W., Naseman, R. W., Platt, T. L., & Lodder, R. A. (2023 a). Potential Process Control Issues With Abatacept. Contact in context, 2023.

Felix, M., Isaacs, J. T., Almeter, P. J., Henderson, B. S., Hunter, A. N., Platt, T. L., & Lodder, R. A. (2023 b). Variability in Content of Hydrocortisone Sodium Succinate. Contact in context, 2023.

Isaacs, J.T., Almeter, P.J., Henderson, B.S., Hunter, A.N., Platt, T.L., & Lodder, R.A. Nonparametric Subcluster Detection in Large Hyperspaces, CIC Computational Sciences, 2023c, 1-24. DOI:10.6084/m9.figshare.23877213

Isaksson, T., & Næs, T. (1988). The effect of multiplicative scatter correction (MSC) and linearity improvement in NIR spectroscopy. Applied Spectroscopy, 42(7), 1273-1284. https://doi.org/10.1366/0003702884429869

Jolliffe, I. T., & Cadima, J. (2016). Principal component analysis: a review and recent developments. Philosophical Transactions of the Royal Society A: Mathematical, Physical and Engineering Sciences, 374(2065), 20150202.

Lodder, R. A., & Hieftje, G. M. (1988). Detection of subpopulations in near-infrared reflectance analysis. Applied spectroscopy, 42(8), 1500-1512.

Matlab. Smoothing Splines. https://www.mathworks.com/help/curvefit/smoothing-splines.html. Retrieved May 28, 2023.

Pollock, D. S. G. (1993). Smoothing with cubic splines. https://www.physics.muni.cz/~jancely/NM/Texty/Numerika/CubicSmoothingSpline.pdf. Retrieved May 28, 2023.

ISSN: 1547-8890